Pharmacophore generation and atom-based 3D-QSAR analysis of substituted aromatic bicyclic compounds containing pyrimidine and pyridine rings as Janus kinase 2 (JAK2) inhibitors

Rajasekhar Chekkara[1,2*], E. Susithra[3], Naresh Kandakatla[1], Venkata Reddy Gorla[1,4] and Sobha Rani Tenkayala[1,4]

[1]*Department of Chemistry, Sathyabama University, Jeppiaar Nagar, Chennai, India*
[2]*GVK Biosciences Pvt. Ltd., Plot No: 79, IDA-Mallapur, Hyderabad, India*
[3]*Faculty of Pharmacy, Sri Ramachandra University, Porur, Chennai, India*
[4]*Department of Chemistry, Dravidian University, Srinivasavanam, Kuppam, India*

_____

ABSTRACT

Janus kinase 2 plays a critical role in JAK/STAT signaling pathways, and has a central role in cell cycle. JAK2 have emerged as a novel therapeutic target of myeloproliferative disorders, autoimmune diseases, essential thrombocytosis, and small molecular inhibition of JAK2 activity developed into an impressive drug target. For a series of JAK2 inhibitors pharmacophore model and atom-based 3D-QSAR models have been developed, to identify the essential structural features required for these JAK2 inhibitors using the PHASE module of Schrodinger. A five featured pharmacophore hypothesis with three hydrogen bond acceptors, one hydrogen bond donor and one aromatic ring provided a best atom-based 3D-QSAR model. The developed 3D-QSAR model have good statistical predictive values as $R^2 = 9659$, $Q^2 = 0.5679$ and effective Pearson R = 0.9405. The results illustrate the structural information of substituted aromatic bicyclic compounds containing pyrimidine and pyridine rings, which might be supportive for further rational design of novel potent Janus kinase 2 inhibitors.

Keywords: Janus kinase 2 (JAK2), pharmacophore model, atom-based 3D-QSAR, PHASE.
_____

INTRODUCTION

Janus kinases, JAK1, JAK2, JAK3 and TYK2 are a family of nonreceptor tyrosine kinases, which plays a critical role in cytokine signaling, growth factor mediated signal transduction, cell proliferation and immune response pathways [1-4]. JAK family members consist of seven JAK homology (JH1-JH7) regions with a C-terminal catalytic domain and a N-terminal FERM domain [5, 6]. Remarkably, Janus kinase 2 has become a significant therapeutic target due to the discovery of single somatic mutation (JAK2 V617F) in pseudokinase (JH2) domain [7], and it's over expression induced constant active JAK/STAT signaling in most of the patents with myeloproliferative disorders [8-10], polycythemia vera (PV) [11], hematologic and solid malignancies [12-14], essential thrombocythemia (ET) [15] and autoimmune diseases [16], etc. These observations invoked various medicinal chemistry and clinical studies in an identification of potent JAK2 inhibitors. At present some of the small molecular inhibitors (namely, Ruxolitinib [17, 18], CYT-387 [19], Pacritinib [20], NS-018 [21], AZD1480 [22], NVP-BSK805 & NVP-BVB808 [23], XL019 [24], CEP701 [25], LY2784544 [26], and others [27]) entered into clinical stage

_____

against myelofibrosis (MF) and other disorders. Hence, development of novel small molecular inhibitors against Janus kinase 2 protein activities has gained importance.

The in-silico molecular modeling studies provide hypothetical information on identification of specific structural features that required for small molecular inhibitors, which play vital roles in biological activity inhibition. The main objective of the present study is to develop pharmacophore models and atom-based 3D-QSAR models for a series of compounds and to determine the required essential structural features against Janus kinase 2 protein activities [28, 29]. PHASE v3.1 [30], which is incorporated in maestro 9.0 (Schrödinger 2009) was used for pharmacophore model and 3D-QSAR model development studies. Due to the common structural frame work of the molecules, we developed atom-based 3D-QSAR models using a dataset of 22 training set and seven test set compounds.
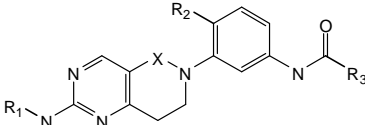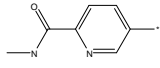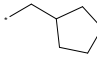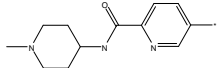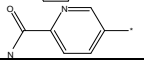
EXPERIMENTAL SECTION

MODELLING METHODS
Dataset
A set of 29 known substituted aromatic bicyclic compounds containing pyrimidine and pyridine rings with JAK2 inhibitory activity were selected for the present study based on a thorough literature survey [31]. The chemical structures of the molecules were drawn using MDL ISIS Draw (Table 1). IC_{50} values were converted into pIC_{50} as shown in Table 2. The total data set molecules were divided randomly into 75% of 22 training set and 25% of seven test set molecules. The randomized division of molecules was done over several runs in order to develop best 3D-QSAR models.

Table: 1 Chemical structure of the dataset molecules

Comp.	R_1	X	R_2	R_3
1	4-(2-(4-methylpiperazin-1-yl)-2-oxoethyl)phenyl	C=O	CH_3	3-(trifluoromethyl)phenyl
2	4-(4-methylpiperazin-1-yl)phenyl	C=O	CH_3	3-(trifluoromethyl)phenyl
3	4-(1-methylpiperidin-4-ylcarbamoyl)phenyl	CH_2	CH_3	3-(trifluoromethyl)phenyl
4	pyrimidin-5-yl	CH_2	CH_3	3-(trifluoromethyl)phenyl
5	4-(pyrrolidine-1-carbonyl)phenyl	CH_2	CH_3	3-(trifluoromethyl)phenyl
6	4-(2-(pyrrolidin-1-yl)ethoxy)phenyl	CH_2	CH_3	5-(trifluoromethyl)thiophene-2-yl
7	4-(2-(pyrrolidin-1-yl)ethoxy)phenyl	CH_2	CH_3	piperidine-1-yl
8	4-(2-(pyrrolidin-1-yl)ethoxy)phenyl	CH_2	CH_3	3,3,3-trifluoro-prop-1-yl
9	4-(4-methylpiperazin-1-yl)phenyl	C=O	Cl	3-(trifluoromethyl)phenyl
10	4-(4-methylpiperazine-1-carbonyl)phenyl	CH_2	CH_3	3,3,3-trifluoro-prop-1-yl
11	4-(N-cyclopropylsulfamoyl)phenyl	CH_2	CH_3	3-(trifluoromethyl)phenyl
12	4-(4-methylpiperazin-1-yl)phenyl	C=O	CH_3	4-(trifluoromethyl)pyridine-2-yl
13	4-(4-methylpiperazine-1-carbonyl)phenyl	CH_2	CH_3	4-(trifluoromethyl)pyridine-2-yl
14	4-(4-methylpiperazine-1-carbonyl)phenyl	C=O	CH_3	4-(trifluoromethyl)pyridine-2-yl
15	4-(4-methylpiperazin-1-yl)phenyl	C=O	Cl	3-fluoro-5-(trifluoromethyl)phenyl
16	4-(4-methylpiperazin-1-yl)phenyl	CH_2	Cl	3-(trifluoromethyl)phenyl
17	4-(methylcarbamoyl)phenyl	CH_2	Cl	3-(trifluoromethyl)phenyl
18	4-(methylcarbamoyl)phenyl	CH_2	Cl	3-fluoro-5-(trifluoromethyl)phenyl
19	4-(methylcarbamoyl)phenyl	CH_2	Cl	4-(trifluoromethyl)pyridine-2-yl
20	4-(4-methylpiperazin-1-yl)phenyl	C=O	CH_3	3-chloro-5-(trifluoromethyl)phenyl
21	4-(4-methylpiperazine-1-carbonyl)phenyl	CH_2	CH_3	3-(trifluoromethyl)phenyl
22	4-(2-(pyrrolidin-1-yl)ethoxy)phenyl	C=O	CH_3	3-(trifluoromethyl)phenyl
23	3-((4-methylpiperazin-1-yl)methyl)phenyl	CH_2	CH_3	3-(trifluoromethyl)phenyl
24	4-(4-methylpiperazin-1-yl)phenyl	C=O	CH_3	3-bromophenyl
25	4-(2-(pyrrolidin-1-yl)ethoxy)phenyl	CH_2	CH_3	cyclopentylamino
26		CH_2	CH_3	3-(trifluoromethyl)phenyl
27	4-(2-(pyrrolidin-1-yl)ethoxy)phenyl	CH_2	CH_3	
28		CH_2	CH_3	3-(trifluoromethyl)phenyl
29		CH_2	CH_3	3-(trifluoromethyl)phenyl

1147

_____

Ligand Preparation
The chemical structure of the dataset molecules were drawn using ISIS Draw. The conversion of chemical structures from 2D to 3D, hydrogen addition and energy minimization of all molecules at OPLS-2005 force field was done by using LigPrep module [32]. For each molecule, a maximum of 2000 conformers were generated using Mixed MCMM/LMOD Search Method as implemented in MacroModel method [33] with an OPLS-2005 force field and distance-dependent dielectric solvent model. All the conformers developed were minimized using TNCG minimization up to 500 iterations. For each molecule, a set of minimized conformers with maximum relative energy difference of 10 kcal/mol was retained at RMSD of 1.00 Å.

Pharmacophore & 3D-QSAR model generation
Pharmacophore model was developed by Phase module, a default structure with six built-in pharmacophore features namely hydrogen bond acceptor (A), hydrogen bond donor (D), hydrophobic group (H), negatively charged group (N), positively charged group (P) and an aromatic ring (R) were applied for creation of pharmacophore sites. The pharmacophore features were interpreted using smarts queries as one of the three possible geometries - Point, Vector or Group representing the physical characteristics of the pharmacophore site. The confirmation of the activity thresholds defined five active compounds ($pIC_{50} >= 8.200$) and 11 inactive compounds ($pIC_{50} <= 7.450$), which are to be used for pharmacophore modeling and subsequent scoring. The common pharmacophores (CPHs) were identified using a tree-based partition algorithm with a maximum tree depth of five with an intersite distance of 2 Å. The final size of pharmacophore box which governs the tolerance on matching was 1 Å. The default scoring hypotheses parameters were applied for examination of the CPHs in order to yield the best alignment of the active ligands.

Atom-based 3D-QSAR models were generated for the selected CPHs using a set of 22 training molecules with a grid spacing of 1.0 Å, random seed value of zero and six PLS factors. The developed 3D-QSAR models were validated by predicting activities of the seven test set molecules.

Table: 2. 3D-QSAR predicted activity of training and test set compounds

Comp.	QSAR Set	Experimental Activity	Predicted Activity	Pharm Set	Fitness Score
1	Training	7.215	7.18	Inactive	2.45
2	Training	7.347	7.36	Inactive	2.46
3	Training	8.155	8.15		2.76
4	Training	7.721	7.64		2.62
5	Test	7.854	7.84		2.63
6	Test	7.745	7.91		2.64
7	Training	7.398	7.43	Inactive	2.65
8	Training	7.678	7.74		2.58
9	Training	8.222	8.1	Active	2.47
10	Training	7.337	7.38	Inactive	2.59
11	Test	7.268	7.78	Inactive	2.52
12	Training	7.319	7.56	Inactive	2.45
13	Training	8.276	8.3	Active	3
14	Training	7.155	7.08	Inactive	2.52
15	Training	8.046	7.98		2.4
16	Test	8.056	8.07		2.82
17	Training	7.824	7.82		2.81
18	Training	8	8		2.68
19	Training	8.194	8.21		2.57
20	Training	7.444	7.44	Inactive	2.38
21	Training	8.523	8.57	Active	2.92
22	Test	7.081	7.42	Inactive	2.37
23	Training	7.553	7.54		2.6
24	Test	7.356	7.69	Inactive	2.43
25	Training	8.398	8.41	Active	2.69
26	Training	7.495	7.49	Inactive	2.66
27	Training	7.921	7.99		2.66
28	Test	8.301	8.22	Active	2.8
29	Training	8.097	7.95		2.77

_____

RESULTS AND DISCUSSION

Pharmacophore modeling and atom-based 3D-QSAR studies were performed on a series of specified organic molecules to determine the importance of specific structural features of JAK2 inhibitors required for the biological activity. The PHASE predicted activity and fitness values were shown in Table 2.

Pharmacophore validation

To generate the common pharmacophore hypothesis, the data set was divided into five active compounds ($pIC_{50} >=$ 8.200) and 11 inactive compounds ($pIC_{50} <= 7.450$) and the rest of the molecules as moderately active with four minimum sites and five maximum sites. We developed 85 five featured CPHs with different combination of variants. From these, five best CPHs namely, AAADR, AADDR, AADHR, ADDHR and ADDRR were chosen for 3D-QSAR model development based on the scoring function and alignment of the active compounds. An atom based 3D-QSAR model was developed to the respective CPHs using twenty two training and seven test molecules with four PLS factors. A summary of quantitative structure-activity relationship (QSAR) results for the five best CPHs is shown in table 3.

Table: 3. Statistical analysis of the selected 3D-QSAR model.

	AAADR	AADDR	AADHR	ADDHR	ADDRR
SD	0.0854	0.0808	0.0477	0.0747	0.0456
R2	0.9659	0.9695	0.9894	0.9739	0.9903
F	120.4	135	395	158.7	433.1
P	3.12E-12	1.22E-12	1.60E-16	3.21E-13	7.39E-17
RMSE	0.2715	0.3176	0.313	0.2726	0.3218
Q2	0.5679	0.4085	0.4253	0.5643	0.3928
Pearson R	0.9405	0.8964	0.6597	0.8422	0.7361

SD, Standard deviation of the regression; R^2, correlation coefficient; F, variance ratio; P, significance level of variance ratio; RMSE, root mean-square error; Q2, predictive coefficient of the test set; Pearson R, Correlation between the predicted and observed activity for the test set.
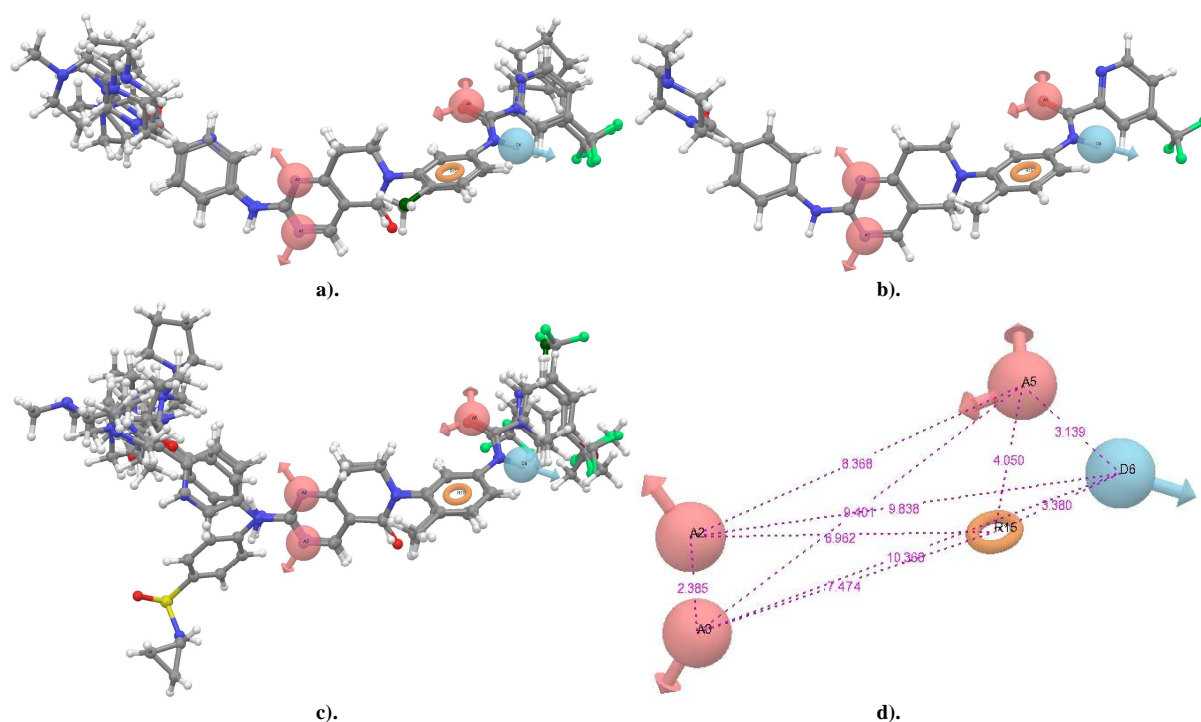

Figure: 1. The best AAADR hypothesis model; a. Alignment of the most active compounds; b. Alignment of the most active compound 13 (highest fitness value = 3); c. Scatter alignment of the inactive compounds; d. Distances between different sites described in Å

The generated five 3D-QSAR models were evaluated using different statistical parameters (R^2, Q^2, SD, RMSE, Pearson R and F) to find the best 3D-QSAR model. The hypothesis AAADR, has shown good R^2 value of 0.9659

_____

for the training set and a predictive potential with Q^2 value of 0.5679, low RMSE value of 0.2715 and highest Pearson R value of 0.9405. Thus, AAADR hypothesis with three hydrogen bond acceptors (A), one hydrogen bond donor (D) and one aromatic ring (R) as pharmacophoric features was selected as the best CPH model. The best hypothesis (AAADR) of the 3D-QSAR model generation is shown in Figure 1. The scatter plot for the predicted and experimental activity of training and test set compounds is shown in Figure 2.
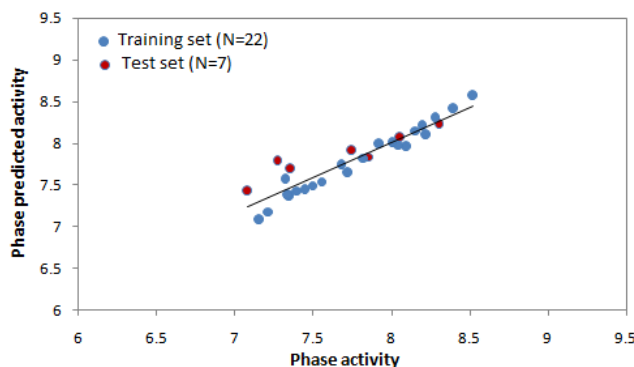

Figure 2. Correlation between predicted (pIC$_{50}$) and phase activity (pIC$_{50}$) of training and test set compounds

QSAR Visualization

The generated counter cubes describe the essential features that play a vital role in interactions between ligand and the active domain of the JAK2 protein. A visual representation of the contours generated for the most active compound 13 and the least active compound 22 is shown in Figure 3 and 4 respectively. In this illustration, blue cubes indicate favourable regions and red cubes indicate unfavourable regions of substituent groups increasing the activity. The cubes generated for different properties such as electron withdrawing, hydrophobic, hydrogen bond donor and combined effect of the most active compound 13 and the least active compound 22 with AAADR hypothesis is shown in Figure 3a-d, Figure 4a-d respectively.
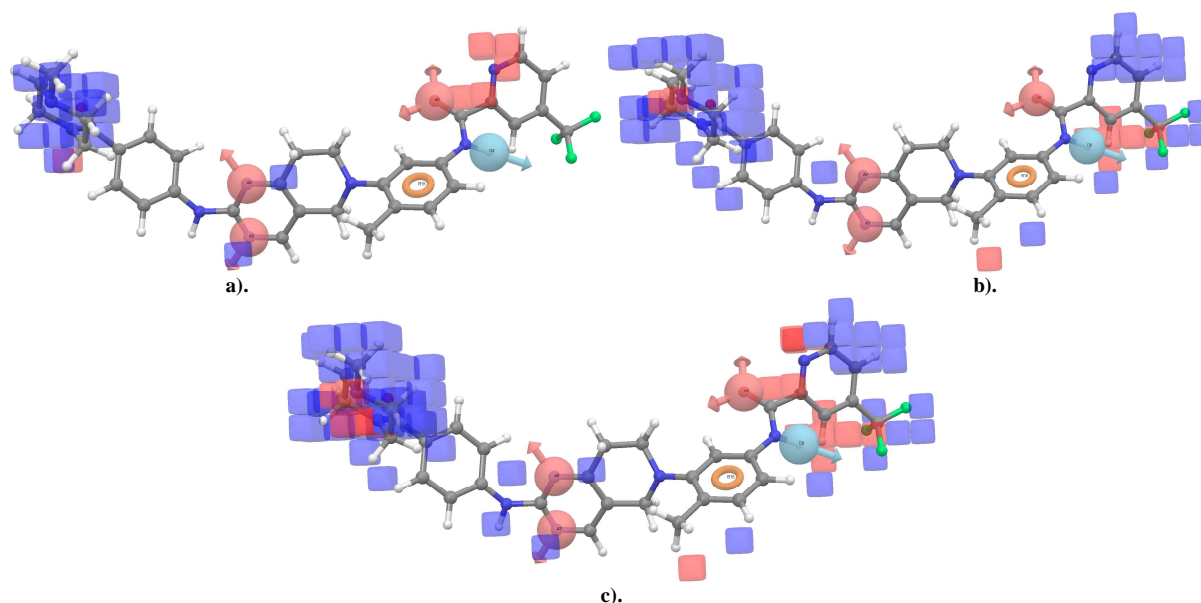

Figure 3. **Atom-based 3D-QSAR model visualization of the most active compound 13 with AAADR hypothesis; a. electron withdrawing feature; b. hydrophobic features and c. combined effect**
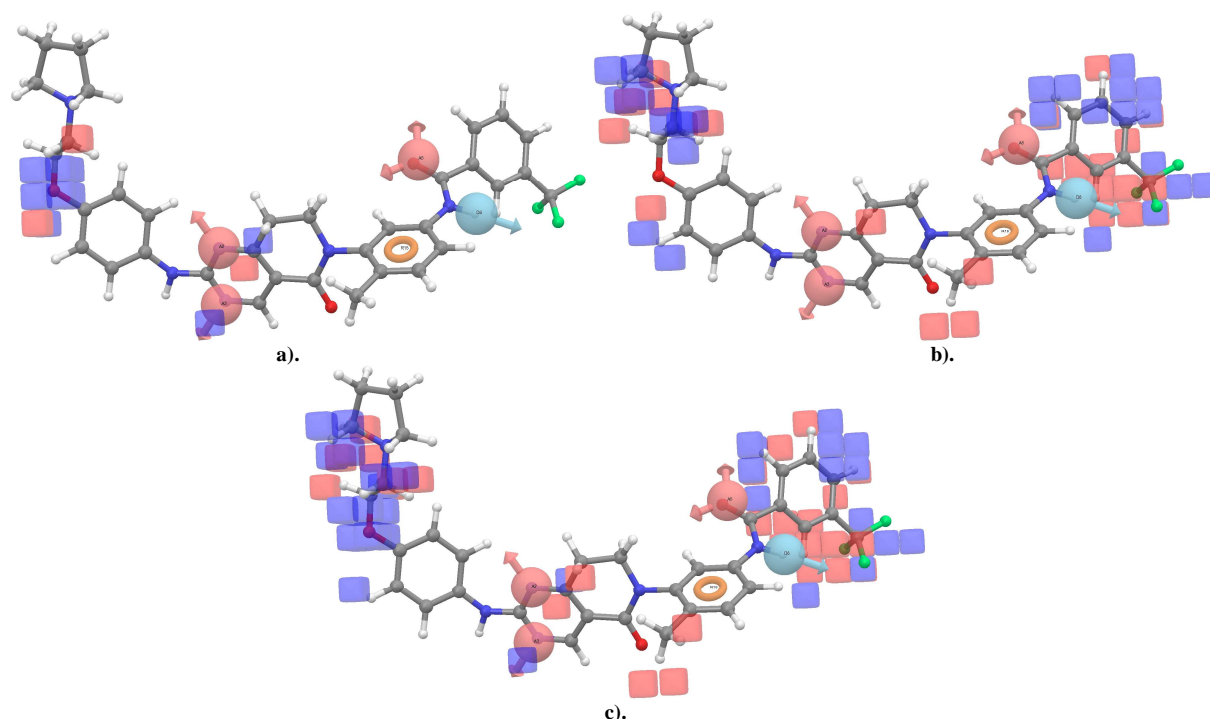
_____

Figure 4. **Atom-based 3D-QSAR model visualization of the least active compound 22 with AAADR hypothesis a. electron withdrawing feature; b. hydrophobic features and c. combined effect**

The contour cubes generated for electron withdrawing features of most active compound 13 (Fig. 3a) reveals the importance of 4-methylpiperazin-1-yl on inhibition of JAK2 activity. The presence of blue cubes at A2 and A3 shows the favorable regions of electron withdrawing features and the substitution of electron withdrawing features at these positions (A2, A3 & 4-methylpiperazin-1-yl group) are acceptable and enhance the activity of the compounds. The addition of electron withdrawing features at pyridine moiety and A5 may not enhance the inhibitory activity of the compounds due to the presence of red cubes, which indicate the unfavorable regions. Fig. 3b, the presence of blue cubes at 4-[(4-methylpiperazin-1-yl)carbonyl] phenyl group attached to the bicyclic ring and trifluoromethylpyridine group attached to carboxamide group represent the favourable regions of hydrophobic features of the compounds. Fig. 3c. illustrates the combined effect of all features of the most active compound, which represents the presence of blue cubes at 4-[(4-methylpiperazin-1-yl)carbonyl]phenyl and trifluoromethylpyridine groups as the favourable regions of the compound.

Likewise, contour cubes generated for electron withdrawing features (Fig. 4a), hydrophobic features (Fig. 4b) and combined features (Fig. 4b) of the least active compound 22 indicate the presence of blue cubes as the favourable regions and also the addition of suitable electron withdrawing groups and hydrophobic groups, respectively, at this positions may enhance the activity of the compound. The red cubes indicate the unfavourable regions of the compound. On comparison of the contour cubes generated for electron withdrawing features and hydrophobic features of the most active 13 and least active 22 compounds, it evidently shows that the presence of 4-[(4-methylpiperazin-1-yl)carbonyl] phenyl and trifluoromethylpyridine groups on bicyclic ring moiety enhance the JAK2 inhibitory activity of the compounds. Due to the lack of above specified groups, compound 22 became less active. Thus, it is recommended that the addition of suitable electron withdrawing groups and hydrophobic groups at the favourable regions (blue cubes) will enhance the activity of the compounds against JAK2 protein.

CONCLUSION

In the present study, several pharmacophore models and atom-based 3D-QSAR models were generated using twenty two training set and seven test set compounds. The generated pharmacophore model has provided a five featured AAADR hypothesis with a highly predictive ability of the JAK2 inhibitors. The developed 3D-QSAR model has provided the structural activity relationship of the compounds by revealing the importance of electron withdrawing

_____

and hydrophobic features on the chemical structure of compounds for the inhibition of JAK2 protein activity. Furthermore, it shows the effect of 4-[(4-methylpiperazin-1-yl)carbonyl] phenyl and trifluoromethylpyridine groups on bicyclic ring moiety with respective JAK2 inhibitory potential of the compounds. Hence, the results obtained from pharmacophore modeling and atom-based 3D-QSAR model presents a theoretical picture in developing newer novel Janus-kinase 2 inhibitors as potential leads in drug design.

REFERENCES

[1] W Vainchenker; SN Constantinescu. *Oncogene*, **2013**, 32(21), 2601-2613.
[2] A Quintas-Cardama; S Vertovsek. *Expert Opin. Invest. Drugs*, **2011**, 20(7), 961-972.
[3] HL Pahl. *Blood*, **2012**, 119(5), 1096-1097.
[4] A Laurence; M Pesu; O Silvennoinen; J O'Shea. *Open Rheumatol. J.*, **2012**, 6(2), 232-244.
[5] K Lindauer; T Loerting; KR Liedl; RT Kroemer. *Protein Eng.*, **2001**, 14(1), 27-37.
[6] M Funakoshi-Tago; S Pelletier; H Moritake; E Parganas; JN Ihle. *Mol. Cell Biol.*, **2008**, 28(5), 1792-1801.
[7] EJ Baxter; LM Scott; P Campbell; C East; N Fourouclas; S Swanton; GS Vassiliou; AJ Bench; EM Boyd; N Curtin; MA Scott; WN Erber; AR Green. *Lancet*, **2005**, 365(9464), 1054-1061.
[8] G Karoline; B Iris; H Claude. *JAK-STAT*, **2013**, 2(3), e25025.
[9] SS Jatiani; SJ Baker; LR Silverman; EP Reddy. *Genes Cancer*, **2011**, 1(10), 979-993.
[10] MR Mamatha; D Anagha; S Martin. *Expert Opin. Ther. Targets.*, **2012**, 16(3), 313-324.
[11] C James. *Hematology Am. Soc. Hematol. Educ. Program*, **2008,** 69-75.
[12] SH Brian; E Gail; J Antonio. *Expert Opin. Invest. Drugs*, **2012**, 21(5), 637-655.
[13] F Yasuko; G Massimo. *Bio Drugs,* **2013,** 27(5), 431-438.
[14] ML Lindsay; LL Ross. *Trends Pharmacol. Sci.*, **2012**, 33(11), 574-582.
[15] A Falanga; M Marchetti; A Vignoli; D Balducci; L Russo; V Guerini; T Barbui. *Exp. Hematol.*, **2007,** 35(5),702-11.
[16] JJ O'Shea; A Kontzias; K Yamaoka; Y Tanaka; A Laurence. *Ann. Rheum. Dis.*, **2013**, 72(2), ii111-ii115.
[17] EW Lowery; SM Schneider. *Clin. J. Oncol. Nurs.*, **2013**, 17(3), 312-318.
[18] HM Kantarjian; RT Silver; RS Komrokji; RA Mesa; R Tacke; CN Harrison. *Clin. Lymphoma Myeloma Leuk.*, **2013,** 13(6), 638-645.
[19] A Pardanani; RR Laborde; TL Lasho; C Finke; K Begna; A Al-Kali; WJ Hogan; MR Litzow; A Leontovich; M Kowalski; A Tefferi. *Leukemia*, **2013**, 27(6), 1322-1327.
[20] E Derenzini; A Younes. *Expert Opin. Invest. Drugs*, **2013**, 22(6), 775-785.
[21] Y Nakaya; K Shide; H Naito; T Niwa; T Horio; J Miyake; K Shimoda. *Blood Cancer J.*, **2014**, 4(1), e174.
[22] BC McFarland; JY Ma; CP Langford; GY Gillespie; H Yu; Y Zheng; SE Nozell; D Huszar; EN Benveniste. *Mol. Cancer Ther.*, **2011**, 10(12), 2384-2393.
[23] F Ringel; J Kaeda; M Schwarz; C Oberender; P Grille; B Dörken; F Marque; PW Manley; T Radimerski; P le Coutre. *Acta Haematol.*, **2014**, 132(1), 75-86.
[24] S Verstovsek; CS Tam; M Wadleigh; L Sokol; CC Smith; LA Bui; C Song; DO Clary; P Olszynski; J Cortes; H Kantarjian; NP Shah. *Leukemia Res.*, **2014**, 38(3), 316-322.
[25] FP Santos; HM Kantarjian; N Jain; T Manshouri; DA Thomas; G Garcia-Manero; D Kennedy; Z Estrov; J Cortes; S Verstovsek. *Blood*, **2010**, 115(6), 1131-1136.
[26] L Ma; B Zhao; R Walgren; JA Clayton; WD Blosser; TP Burkholder; MC Smith. *Ann Meet Abstr.*, **2010**, 116(21), 4087.
[27] CS Tam; S Verstovsek. *Expert Opin. Invest. Drugs*, **2013**, 22(6), 687-699.
[28] D Singh Kh; M Karthikeyan; P Kirubakaran; S Nagamani. *J. Mol. Graph. Model.*, **2011,** 30, 186-97.
[29] X Wu; S Wan; J Zhang. *Int. J. Mol. Sci.*, **2013,** 14(6), 12037-12053.
[30] PHASE, version 3.1., **2009,** Schrödinger, LLC, New York, NY, USA.
[31] MC Andres; M Murone; S Sengupta; SJ Shetty. *WO Patent,* **2011**, 101806A1.
[32] LigPrep, Version 2.3., **2009**, Schrodinger, LLC, New York, NY.
[33] MacroModel., version 9.7., **2009,** Schrödinger, LLC, New York, NY, USA.